The role of copper speciation in the low temperature oxidative upgrading of short chain alkanes over Cu/ZSM-5 catalysts

Robert D. Armstrong[a], Virginie Peneau[a], Nadine Ritterskamp[a], Christopher J. Kiely[b], Stuart. H. Taylor[a] and Graham J. Hutchings[a]*

Abstract: Partial oxidative upgrading of C_1 – C_3 alkanes over Cu/ZSM-5 catalysts prepared by chemical vapour impregnation (CVI) has been studied. The undoped ZSM-5 support is itself able to catalyse selective oxidations, for example, methane to methanol, using mild reaction conditions and the green oxidant H_2O_2. Addition of Cu suppresses secondary oxidation reactions, affording methanol selectivities of up to 97 %. Characterisation studies attribute this ability to population of specific Cu sites below the level of total exchange (Cu/Al < 0.5). These species also show activity for radical- based methane oxidation, with productivities exceeding those of the parent zeolite supports. When tested for ethane and propane oxidation reactions, comparable trends are observed.

Introduction

Finite crude oil reserves and increasingly environmentally-conscious legislation are driving the search for alternate feedstocks and routes for the synthesis of bulk chemical products. Proposed as a transitional fuel for the move away from a petroleum- derived economy, the valorisation of natural gas as a chemical feedstock is therefore a key field of research. Comprising mainly methane and ethane, the direct oxidation of these lower alkanes is hindered by their kinetically inert nature, with C-H bond energies of 439.57 and 423.29 kJ mol^{-1} [1]. As a result, commercialised technologies often use indirect routes and are energy intensive. For instance, syngas is required for the methanol synthesis process, and is produced through steam reforming of methane [2]. Through carbonylation at high pressures of carbon monoxide, methanol then yields an estimated 75% of global acetic acid (*ca* 7.8 Mt/annum) via the BP Cativa and Celanese processes [3-5]. Meanwhile steam cracking of ethane yields ethene, a precursor to ethanol, acetaldehyde, acetic acid and polyethylene amongst other higher value products [6]. The direct oxidation of short chain alkanes to partially oxygenated products is therefore economically and environmentally preferable to current practices.

In nature, methane monooxygenase (MMO) oxidises n-alkanes selectively to alcohols under ambient conditions, over a μ-oxo bridged diiron active site [7, 8]. Synthetic approaches to directly oxidise these lower alkanes have been reported, and typically fall into three categories; (i) gas phase systems – typically at high temperatures and/ or pressures [9-16], (ii) biomimetic- structural models of MMO active site [17, 18] and (iii) oxidation in acidic media to produce methyl/ ethyl esters [19-23]. It should be noted that transition metal- containing materials have also been activated in N_2O/O_2 and subsequently used to oxidise alkanes, though not in a truly closed catalytic cycle [24, 25].

It has recently been reported that ZSM-5 shows high intrinsic activity in the low temperature oxidation of C_1 – C_3 alkanes with hydrogen peroxide as oxidant [26-29]. Hammond *et al.* attributed catalytic activity to trace amounts of iron, present as impurities within the zeolite [26, 30]. These are shown to form catalytically active extra-framework diiron- μ- oxo- hydroxo or oligomeric iron complexes upon high temperature activation [26, 30]. Addition of Cu^{2+} was shown to afford high selectivity to methanol (*ca.* 90%) by inhibiting further oxidation to formic acid, with no overall change in catalyst productivity [26]. This effect was shown when Cu was introduced as a homogeneous additive, a supported co-catalyst or supported upon ZSM-5 itself. Through EPR spectroscopy experiments, this effect was shown to be due to a lack of hydroxyl radicals when Cu^{2+} was present [26, 31]. A shift in reaction selectivity was also reported for ZSM-5 (SiO_2/Al_2O_3 = 30) catalysed ethane oxidation upon addition of Cu^{2+}, though rather than affording high ethanol selectivity as might be expected from C_1 studies, this led to lower acetic acid and high ethene selectivity (> 30 %) [27]. Mechanistic studies showed that ethane is activated to yield two primary products; ethylhydroperoxide and ethanol, with ethene also indicated as a potential primary product. These were shown to undergo catalytic oxidation to acetic acid, with C-C scission yielding C_1 oxygenates; formic acid, methylhydroperoxide and methanol [27]. Oxygenate selectivity was consistently high (*ca*. 95 %) [27]. Concordantly, high propene selectivities were observed when the same catalysts were tested for propane oxidation under comparable conditions [32].

The aim of the present work is to study the role that Cu speciation plays in effecting the performance of Cu/ZSM-5 catalysts. To this end we characterise Cu/ZSM-5 catalysts using DR-FTIR, TEM, TPR and NH_3-TPD to identify specific Cu sites and correlate these with catalyst performance. Through EPR trapping studies we then aim to rationalise testing and characterisation data to determine structure – function relationships. We aim to determine whether Cu sites perform in the same way during the catalytic oxidation of methane, ethane and propane with H_2O_2.

Results and Discussion

Studies into the selective oxidation of methane to methanol using supported ZSM-5 (30) catalysts have reported increased reaction

[a] Cardiff Catalysis Institute
School of Chemistry, Cardiff University
Park Place, Cardiff, UK, CF10 1AQ
Corresponding E-mail: Hutch@Cardiff.ac.uk
[b] Department of Materials Science and Engineering,
Lehigh University, 5 East Packer Avenue, 18015-3195, Bethlehem, Pennsylvania, USA

Supporting information for this article is given via a link at the end of the document.((Please delete this text if not appropriate))

selectivity in the presence of Cu^{2+}, with no loss of reaction rate. In that system EPR studies showed that Cu^{2+} was either (i) suppressing the propagation of •OH or (ii) catalytically sequestering ·OH and therefore affording high primary product selectivity [26, 31]. Our previous studies into ZSM-5 (30) to catalysed ethane oxidation determined that ethene was formed under reaction conditions, with particularly high selectivity observed upon testing of 2.5 Cu/ZSM-5 (30) and 1.25% Fe 1.25% Cu/ZSM-5 (30) catalysts (30.2 and 34.2 % selectivity respectively)[27]. It was concluded that ethene could form through two pathways; (i) direct H-abstraction from the alkane or (ii) a fully concerted mechanism over $[Fe=O]^+$ [27]. It was suggested that ethane undergoes activation at the iron sites in ZSM-5 to yield ethene. Ethene can then undergo oxidation or, in the presence of Cu^{2+} desorb from the zeolite surface and diffuse to the liquid- gas interface. Indeed, ethene was shown to undergo catalytic oxidation under reaction conditions, yielding the reaction products; formic acid, CO_x and CH_3OOH/ CH_3OH [27].

The reactivity of ethene under test conditions is further explored in Table S1. Addition of Cu to either H-ZSM-5 (30) or 1.25% Fe/ZSM-5 (30) led to no significant change in the rate of H_2O_2 conversion. However, when Cu was present, the rate of ethene oxidation typically decreased. For example, deposition of 2.5 wt% Cu onto H-ZSM-5 (30) effected a decrease in the rate of ethene oxidation from 1.2 to 0.6 $mol_{Ethene\ converted}\ kg_{cat}^{-1}\ h^{-1}$ (Table 1, Entries 2 and 4). Also, whilst selectivity favoured C_1 products, Cu-containing catalysts afforded appreciable yields of acetic acid (Table S1, Entries 5 and 7). Given that the oxidation of ethene to acetic acid is well documented [33, 34] it can be concluded that ethene is a primary product in this reaction. Indeed, the reactivity of ethene in this system is comparable to that of methanol under analogous conditions.

ZSM-5 catalysed alkane oxidation reactions

Cu/ZSM-5 catalysts prepared by CVI were tested for the oxidation of methane under mild aqueous conditions, utilising hydrogen peroxide as the oxidant. Although higher rates of methane activation might be attained through co-impregnation of the ZSM-5 supports with Fe, the presence of Fe species would prevent specific characterisation of Cu sites [26]. In line with previous studies, a metal loading of 2.5 wt% Cu was employed [26], whilst the SiO_2/Al_2O_3 ratio was varied within the range of 23 – 280. Reaction data at t = 0.5 h are presented in Table 1 (Entries 1-4). Of the catalysts tested, 2.5% Cu/ZSM-5 (SiO_2/Al_2O_3 = 23) showed relatively high activity, with 42.8 µmol products formed and 97.4 % selectivity towards methanol. This is compared with the previously reported 2.5 % Cu/ZSM-5 (30), which yielded 8.4 µmol products at 78.5 % methanol selectivity. Further increasing the SiO_2/Al_2O_3 to 50 or 280 (at a fixed loading of 2.5 wt. % Cu) led to further decreases in catalyst activity. Higher SiO_2/Al_2O_3 showed a significant change in colour post- reaction, with 2.5% Cu/ZSM-5 (30-280) turning yellow (Figure S2). This is consistent with formation of reduced Cu species, potentially Cu-OOH. Notably, 2.5% Cu/ZSM-5 (23) showed no apparent colour change. Alumina- free 2.5 % Cu/Silicalite-1 (Table 1, Entry 13) showed relatively low productivity (4.3 µmol) and methanol selectivity (52.9 %) despite a higher rate of H_2O_2 conversion. To rationalise these data, proton form H-ZSM-5 (SiO_2/Al_2O_3 = 23 or 30) were assessed for activity (Table 1, Entries 5 and 9). Of these unmodified zeolites, H-ZSM-5 (30) showed markedly higher rates of methane conversion (2.1 mol $kg_{cat}^{-1}\ h^{-1}$) than H-ZSM-5 (23)(0.51 mol $kg_{cat}^{-1}\ h^{-1}$) which is consistent with previous studies [26]. This despite ICP-MS analysis showing the calcined zeolites to contain comparable levels of Fe contamination (140 and 120 ppm for ZSM-5 23 and 30 respectively). The trend towards increasing oxygenate yield with decreasing SiO_2/Al_2O_3 in Table 1, indicates a potential role of the zeolite support in effecting not only the catalytic activity but also selectivity. Indeed, this would be consistent with the proposed extra-framework diiron- µ- oxo-hydroxo active site being stabilised/ sited at AlO_4^- exchange sites [26], the concentration of which increase with decreasing Si/Al. The speciation of Cu would also be expected to differ upon varying the composition of these MFI zeolites, as has been extensively reported [35-37]. Copper species are known to catalyse a myriad of reactions in the presence of H_2O_2 [38, 39], therefore data in Table 1 might also indicate formation of a Cu species which is capable of propagating radical- based methane oxidation. To better understand the role which Cu sites might play in effecting the differing rates of methane conversion and methanol selectivities observed for Cu/ZSM-5 catalysts in Table 1, the physicochemical properties were fully characterised.

Transmission electron micrographs for 2.5% Cu/ZSM-5 catalysts are shown in Figure 1. A strong support effect was observed for this group of catalysts. With increasing SiO_2/Al_2O_3 ratio we observed a steady decrease in the mean particle size of supported Cu species, from 9.0 nm for ZSM-5 (23) to 2.0 for ZSM-5 (280). Across the same range the particle size distribution

Table 1 Catalytic data for methane oxidation catalysed by Cu/ZSM-5 of varied SiO_2/Al_2O_3 and Cu/Al ratios.

Entry	SiO_2/ Al_2O_3	% wt Cu	Cu/Al ratio	Total Product / µmol	Product / µmol				χ H_2O_2 / %	*S*(MeOH) / %
					MeOH	MeOOH	HCOOH	CO_2		
1	23	2.5	0.41	42.82	41.7	0.57	0	0.55	8.68	97.38
2	30	2.5	0.59	8.37	6.57	1.29	0	0.51	2.48	78.49
3	50	2.5	0.76	0.52	0.00	0.14	0	0.38	1.83	0.00
4	280	2.5	4.08	2.2	0.43	1.43	0	0.34	11.40	19.55
5	23	0	n.a	6.91	1.14	5.43	0	0.34	0.08	16.50
6	23	0.4	0.07	40.23	37.71	2.14	0	0.38	1.08	93.74
7	23	1.25	0.20	51.89	49.86	1.43	0	0.60	2.10	96.09
8	23	5	0.82	1.38	0.43	0.43	0	0.52	6.76	31.16
9	30	0	n.a	28.15	5.14	14.57	7.43	1.01	13.14	18.26
10	30	0.4	0.09	44.96	32.86	9.29	0	2.82	7.96	73.08
11	30	1.25	0.29	48.83	42.00	4.29	0	2.52	2.10	86.01
12	30	5	1.18	5.29	3.14	1.71	0	0.44	11.52	59.36
13[a]	n/a	2.5	n/a	4.33	2.29	1.14	0	0.90	20.55	52.89

Test conditions; 27 mg catalyst, 0.5 h, P(CH_4) = 30 bar (0.03 mol), 50 °C, 1500 rpm, [H_2O_2] = 0.5 M (5000 µmol). [a] Catalyst – 2.5% Cu/Silicalite-1 (CVI)

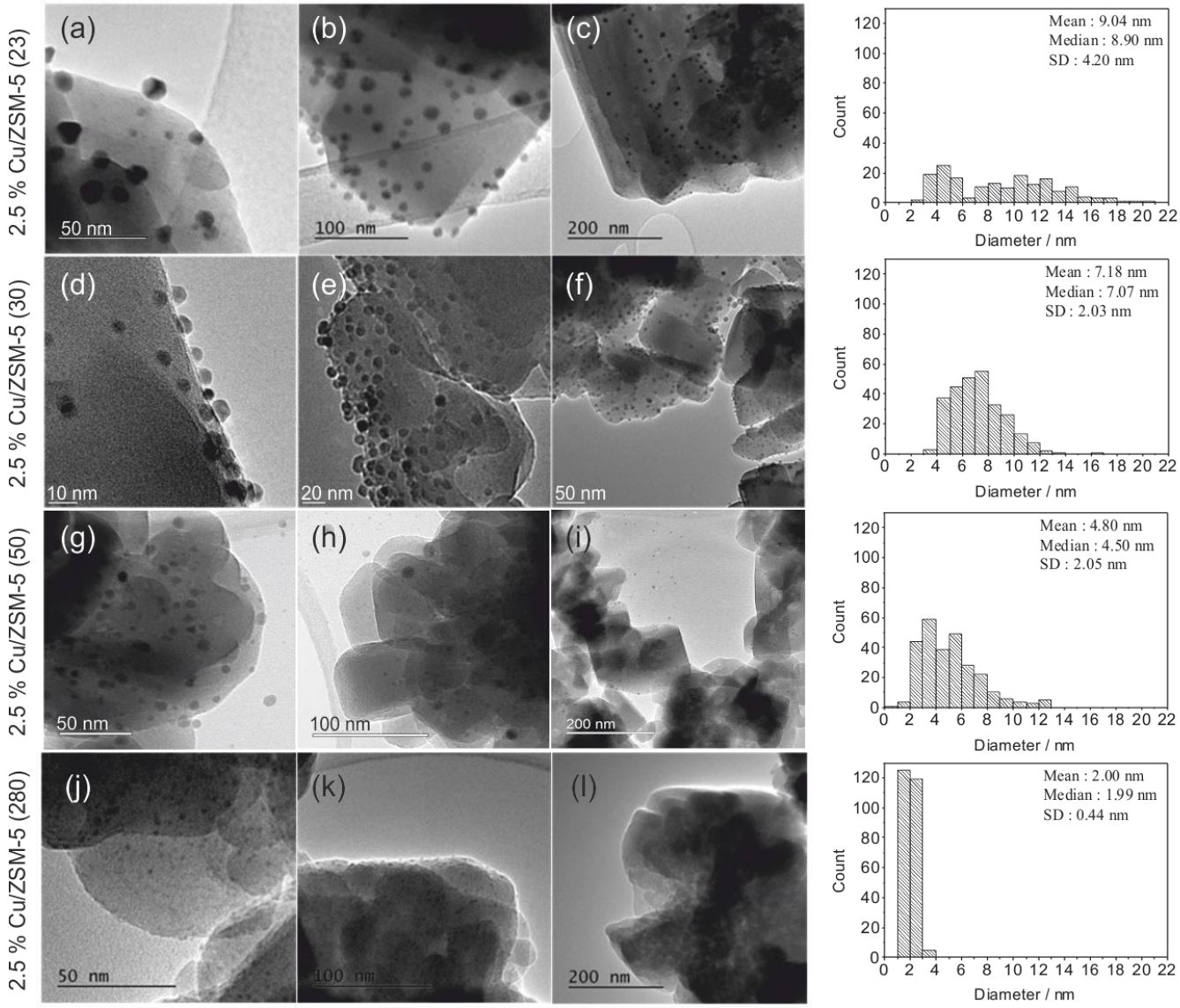

Figure 1 Representative transmission electron micrographs and corresponding particle size distributions for 2.5 wt% Cu supported on; ZSM-5 (23) (a,b,c), ZSM-5 (30) (d,e,f), ZSM-5 (50) (g,h,i) and ZSM-5 (280) (j,k,l).

converged, with a standard deviation in particle size of 4.20 nm and 0.44 nm for ZSM-5 (23) and ZSM-5 (280) respectively. Such an effect has not, to our knowledge, been reported for Cu/ZSM-5 catalysts. We attribute this relationship between alumina content and copper oxide particle growth to varying degrees of interaction between the hydrophobic Cu $(acac)_2$ precursor and the zeolite surface. With increasing SiO_2/Al_2O_3 ratio, ZSM-5 becomes more hydrophobic and this would lead to a stronger interaction with Cu $(acac)_2$. Owing to the lack of solvent, and associated diffusion and pH effects, this might therefore be unique to the CVI methodology. Such particle size- control presents an intriguing avenue for future research, assuming that it might be generalised to other supports and metal- acetylacetonates. Average particle size appears to correlate with the activity and selectivity of these catalysts, however a role for exchanged cationic copper species cannot be excluded.

H_2-TPR was employed to probe the reducibility of Cu species in the 2.5% Cu/MFI zeolite catalysts. H_2 uptake plots are shown in Figure 2. All samples exhibit a low temperature reduction (R_1) at *ca*. 183 – 213 °C, which has been reported to comprise of two simultaneous reductions (i) reduction of isolated Cu^{2+} ions and Cu^{2+} oxocations to Cu^{+} and (ii) reduction of Cu^{2+} in CuO to Cu^0 [40-45]. 2.5% Cu/ZSM-5 catalysts present a second high temperature peak (R_2), not shown for the Silicalite-1 catalyst, which is attributed to the reduction of Cu^{+} ions to Cu^0 [40, 41, 44-47]. The maxima of R_1 and R_2 shifted to a higher temperature with decreasing SiO_2/Al_2O_3. This is generally ascribed to a change in dispersion and increasing interaction between Cu^{n+} species with framework oxygen as the zeolite matrix becomes more negatively charged (higher Al content) [41, 44, 46]. The increasing breadth of R_2 with decreasing SiO_2/Al_2O_3 suggests the presence of oligomeric Cu species of varying nuclearity [45] and is consistent with the broadening particle size distribution of surface oxides shown in Figure 1.

As H_2-TPR studies suggested the presence of exchanged Cu^{2+} species, the occupation of exchange sites was confirmed through

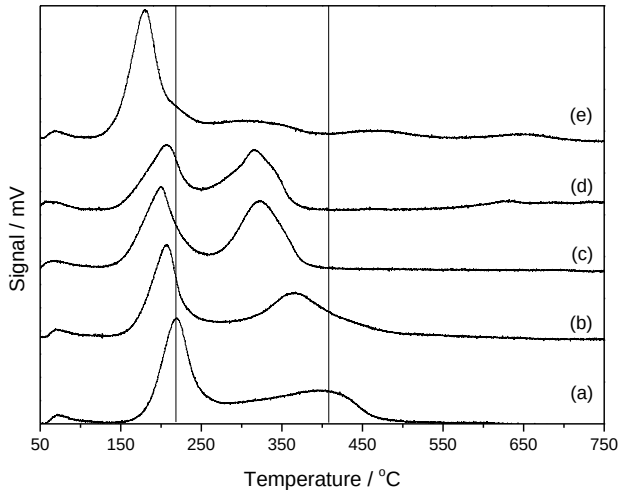

Figure 2 H_2-TPR profiles for 2.5% Cu/ MFI zeolite catalysts prepared by chemical vapour impregnation. (a) ZSM-5 (23), (b) ZSM-5 (30), (c) ZSM-5 (50), (d) ZSM-5 (280) and (e) Silicalite-1

NH_3-TPD and FTIR in the O-H stretching region. TPD plots and FTIR spectra for H-ZSM-5 and 2.5% Cu/ZSM-5 catalysts (SiO_2/Al_2O_3 = 23, 30, 50 and 280) are presented in Figure 3. Two key NH_3 desorptions were observed for all catalysts in Figure 3i, centred at *ca*. 270 and 450 ºC. The lower temperature desorption is attributed to adsorption at weak acid sites (Brønsted and Lewis) with the high temperature desorption unequivocally assigned to NH_3 chemisorbed at strongly acidic Brønsted sites [48-54]. All zeolites showed decreased NH_3 capacity following Cu impregnation, averaging a loss of 26.0 % (± 5.4 %) of total strong-Brønsted sites. This was supported by DRIFTS spectra in Figure 3ii which showed decreased intensity of the peak at 3607 cm^{-1} (OH groups coordinated to Td framework Al^{3+}) for each ZSM-5 following Cu impregnation [55]. NH_3-TPD and DRIFTS therefore suggest siting of Cu^{n+} at AlO_4^- exchange sites.

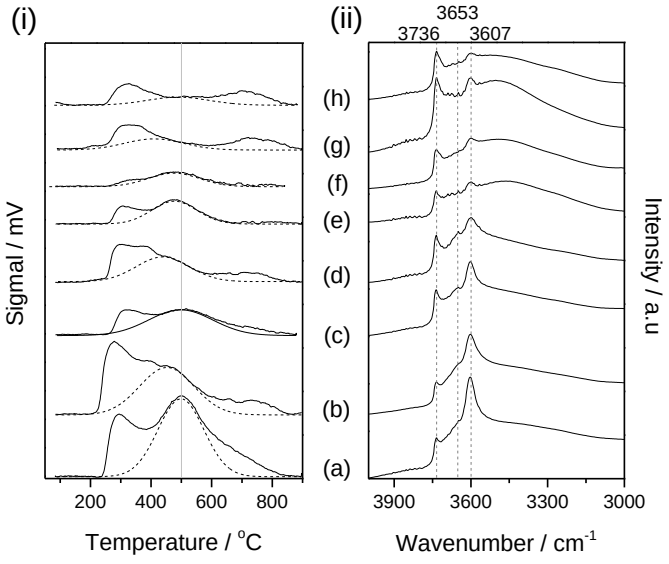

Figure 3 NH_3-TPD traces (i) and DRIFTS spectra in the OH vibrational region (ii) for (H-ZSM-5, 2.5% Cu/ZSM-5) respectively where SiO_2/Al_2O_3 = 23 (a,b), 30 (c,d), 50 (e,f) and 280 (g,h). For (i) dashed lines – peak fit of high temperature desorption.

Cu^{n+} speciation in Cu/ZSM-5 has long been studied due to its activity in the catalytic decomposition or reduction of NO_x, with highly reducible, isolated Cu^{2+} found to be the preferred active site [35, 37, 56-58]. In probing ion exchanged Cu sites with NO, spectroscopically distinct N-O IR stretching bands have been identified, and shown to arise from binding to Cu^{2+} in differing coordination environments [35, 37, 47, 59-63]. Four principle N-O-Cu^{2+} binding modes have been described, differing in geometry and the number of local AlO_4^- exchange sites. These consist of exchanged divalent Cu^{2+} of; square pyramidal (AlO_4^- pair, 1913 cm^{-1}, denoted *Cu-I*), square planar (single AlO_4^-, 1895 cm^{-1}, *Cu-II*), square pyramidal (AlO_4^- pair, 1921 cm^{-1}, *Cu-III*) and *unassigned* (low intensity, 1906 cm^{-1}, *Cu-IV*) geometries [36, 59]. Additional bands at 1813 cm^{-1} (monovalent Cu^+-NO species) and 1875 cm^{-1} (low intensity, gaseous NO) have also been reported [35, 36, 64].

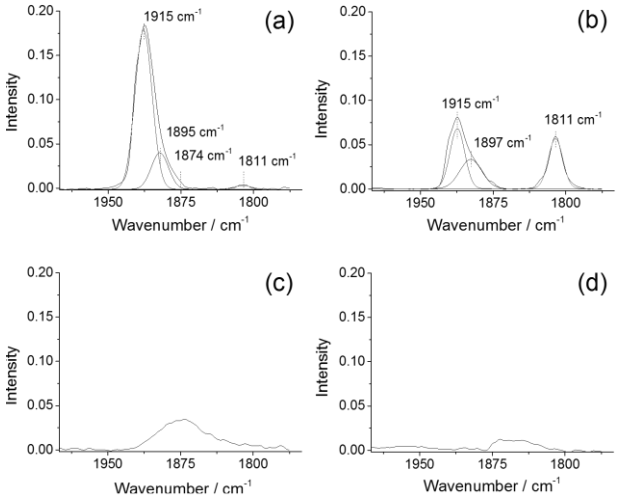

Figure 4 IR bands of NO adsorbed onto 2.5 wt% Cu/ZSM-5 of varying SiO_2/Al_2O_3. SiO_2/Al_2O_3 being (a) 23, (b) 30, (c) 50 and (d) 280.

Spectra acquired following NO saturation of 2.5% Cu/ZSM-5 (SiO_2/Al_2O_3 = 23-280) are shown in Figure 4. The absolute absorbance decreased with increasing SiO_2/Al_2O_3, suggesting a decreasing concentration of exchanged Cu species. Indeed, this was consistent with NH_3-TPD results which showed occupation of *ca.* 26% of strong Brønsted sites for all zeolites, independent of total acidity. Curved fitted spectral bands for 2.5% Cu/ZSM-5 (23) (a) and 2.5% Cu/ZSM-5 (30) (b) are presented, whilst absorbance in (c) and (d) wasn't sufficiently intense to allow for objective fitting. Four bands were identified in (a) and (b), centred at; 1915, 1895, 1874 and 1811 cm^{-1}. The distribution of Cu sites shifted with an increasing Cu/Al ratio (0.41 and 0.59 for ZSM-5 23 and 30 respectively) with increased relative intensity of bands at 1895 cm^{-1} and 1811 cm^{-1} over that at 1913 cm^{-1}. This is consistent with previous reports which showed that Cu-I type sites (AlO_4^- pair, 1913 cm^{-1}) are favourable at low Cu/Al ratios, with Cu-II (1895 cm^{-1}) becoming dominant when overexchanged at Cu/Al > 0.5. It has also been reported that Cu-II type species undergo more facile reduction due to the low local negative charge, which results from being bonded to an isolated AlO_4^- site [35, 65]. In fact, the band at 1811 cm^{-1} (Cu^+-NO) is believed to result from autoreduction of Cu-II (1895 cm^{-1}), resulting from dehydration during the pre-treatment [35, 66].

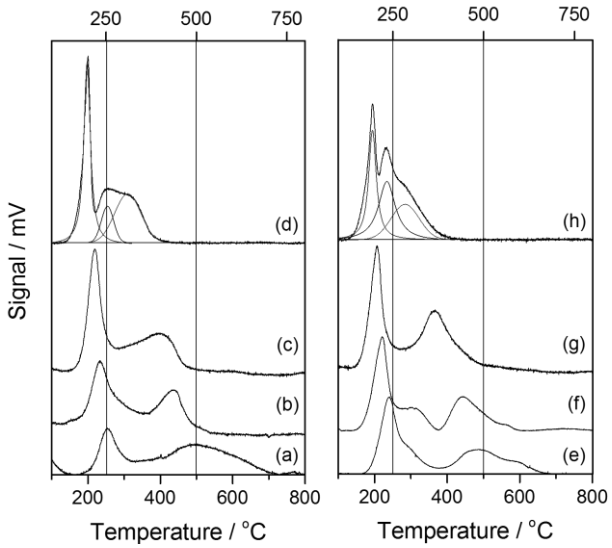

Figure 5 H_2-TPR profiles for Cu/ ZSM-5 of varying Cu/Al. (a) 0.4% Cu/ZSM-5 (23), (b) 1.25% Cu/ZSM-5 (23), (c) 2.5% Cu/ZSM-5 (23), (d) 5% Cu/ZSM-5 (23), (e) 0.4% Cu/ZSM-5 (30), (f) 1.25% Cu/ZSM-5 (30), (g) 2.5% Cu/ZSM-5 (30), (h) 5% Cu/ZSM-5 (30)

Clearly the nature of supported Cu species, both surface oxides and ion exchanged, varied greatly with SiO_2/Al_2O_3 ratio (at a constant 2.5 wt % loading). This made determining the exact catalytic site difficult. Added to this, one had to consider the hydrophobic/ hydrophilic nature of the support itself as rapid diffusion of products out of the zeolite pores is expected to afford higher selectivity towards primary products. Indeed it has been shown that a hydrophobic-hydrophilic shift occurs at a SiO_2/Al_2O_3 ratio of *ca.* 20 [67, 68]. To decouple the effects of zeolite hydrophilicity, surface oxide dispersion and exchange capacity, H-ZSM-5 with a SiO_2/Al_2O_3 of 23 and 30 were impregnated with 0.4 – 5 wt % loadings of Cu.

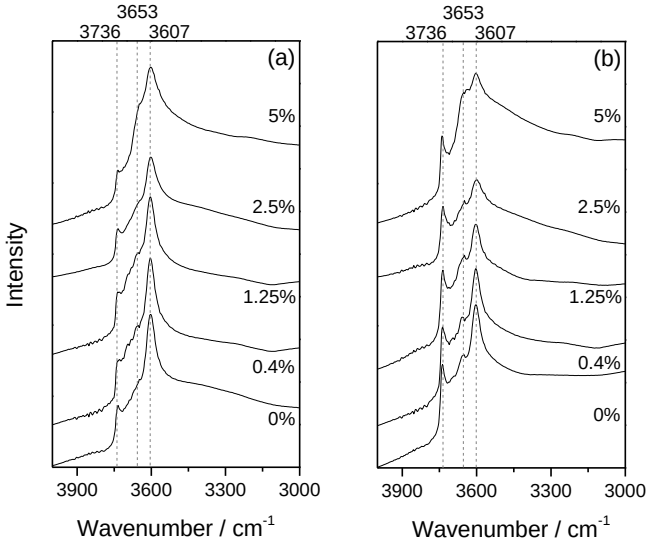

Figure 6 DRIFTS spectra in the OH vibrational region for Cu/ZSM-5 catalysts of varying Cu loading on (a) H-ZSM-5 (23) and (b) H-ZSM-5 (30). (30), (g) 2.5% Cu/ZSM-5 (30), (h) 5% Cu/ZSM-5 (30)

These materials were tested for catalytic activity in methane oxidation and testing data is shown in Table 1. At Cu loadings of 0.4 and 1.25 wt. %, ZSM-5 (23) and ZSM-5 (30) catalysts show comparable productivities. Indeed, at 1.25 wt. % Cu, 51.9 µmol and 48.8 µmol of products were observed for ZSM-5 (23) and ZSM-5 (30) respectively. Methanol selectivity was higher for the more aluminous catalyst (96.1 % vs 86.0 %). Methane conversion, though low, increased with Cu loading for both zeolites which is consistent with copper's ability to catalyse H_2O_2 conversion [69-71]. However once the Cu/Al ratio exceeded 0.5, both methane conversion and methanol selectivity were observed to decrease significantly. To determine whether the step change in activity observed between loadings of 2.5 and 5 wt. % Cu was due to pore blocking by Cu species, N_2 adsorptions studies were carried out (Table S2). A steady decrease in surface area was observed with increasing Cu loading, from 423 m^2g^{-1} for the parent zeolite to 259 m^2g^{-1} at 5 wt. % Cu loading (Table S2, Entries 1 and 5). Despite showing markedly different catalytic performance, 2.5% and 5 % Cu/ZSM-5 (23) catalysts show similar micropore volumes (0.10 and 0.09 cm^3g^{-1} respectively), suggesting that pore blockage is not a key factor.

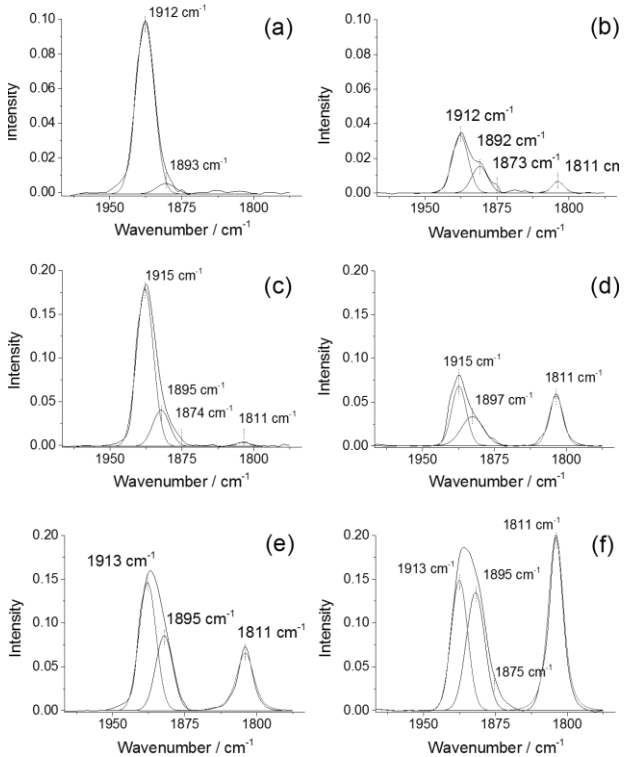

Figure 7 IR bands of NO adsorbed onto Cu(II) and Cu(I) sites in Cu/ZSM-5 of varying Cu/Al. (a) 1.25% Cu/ZSM-5 (23), (b) 1.25% Cu/ZSM-5 (30), (c) 2.5% Cu/ZSM-5 (23), (d) 2.5% Cu/ZSM-5 (30), (e) 5% Cu/ZSM-5 (23) and (f) 5% Cu/ZSM-5 (30).

Cu/ZSM-5 (23) and (30) catalysts of increasing Cu wt. loadings were studied using H_2-TPR (Figure 5), at constant mol_{Cu}. As in Figure 2, two main reduction peaks were observed, at *ca*. 194 – 308 °C (R_1) and 310 – 507 °C (R_2), which may be assigned as previously. Consistent with Figure 4, the T_{max} for both reduction peaks shifted to a lower temperature with increasing Cu/Al (either through increased Cu loading or decreased Al content). At the highest loading (5 wt % Cu) a third reduction event was observed, with T_{max} of 256 and 233 °C for ZSM-5 (23) and ZSM-5 (30) respectively. This is assigned as a low temperature Cu^+- Cu^0

reduction where Cu^{2+} of type Cu-II have undergone auto-reduction to Cu^{+} during the pretreatment. Cu/ZSM-5 (23) catalysts of 0.4 and 5.0 wt. % Cu loading were analysed using HRTEM. Representative micrographs are shown in Fig. S3. At 0.4 wt. % Cu loading (Fig S3a) no discreet nanoparticles were observable. However, upon prolonged exposure to the electron beam (Fig S4) apparent nanoparticle formation was observed. This indicates (a) sintering of Cu- species of a size below the sensitivity of the microscope (sub 1 nm), or (b) migration of nanoparticles from deep within the zeolite pores. At 5.0 wt. % Cu loading, a mean particle size of 4.78 nm was observed (Fig. S3a/c). Consideration of particle size data from Figures 1 and S3 alone, with catalyst performance in Table 1 is paradoxical. At a fixed 2.5 wt. % Cu loading, decreasing average NP size (increasing SiO_2 / Al_2O_3) correlated with decreasing catalytic activity (Fig. 1). Conversely, a decrease in activity is observed with increasing Cu loading despite apparent increases in average NP size (Fig S3). This contradiction further indicates that the nature/ distribution of ion exchanged Cu- species is the key feature which effected the trends observed in Table 1 and not Cu-oxide crystallite size.

DRIFTS spectra for these catalysts are shown in Figure 6. These clearly show a decrease in the intensity of the peak at 3607 cm^{-1} (OH groups coordinated to Td framework Al^{3+}) with increasing Cu loading, and this is consistent with a gradual increase in the degree of cation exchange/ population of Cu^{n+} species [55].

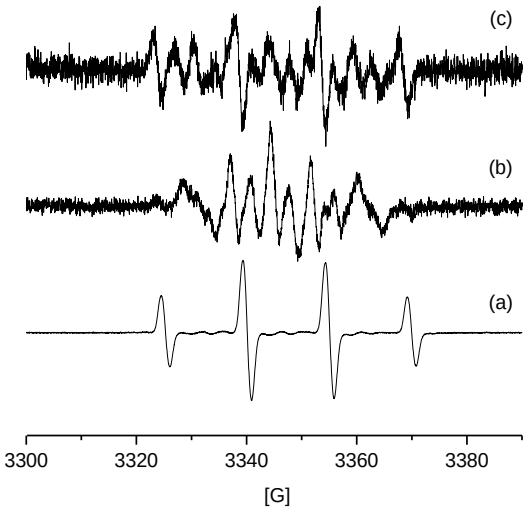

Figure 8 DMPO spin- trapping data obtained during a methane oxidation reaction catalysed by (a) 2.5 % Cu/ZSM-5 (23), (b) 2.5 % Cu/ZSM-5 (30) and (c) 2.5% Cu/ZSM-5 (280) Reaction conditions; 27 mg catalyst, 50 ^{o}C, 5 min, [H2O2] = 0.5 M (5,000 µmol), 1500 rpm P(CH_4) = 30 bar.

As before, the distribution of Cu^{n+} sites was probed using NO-DRIFTS. Spectra for loadings of 1.25, 2.5 and 5 wt % Cu/ ZSM-5 (23 and 30) are shown in Figure 7. For both ZSM-5 (23) and (30) an increase in Cu loading was accompanied by increased absorbance and a shift in the distribution of Cu^{n+} species. Increased Cu/Al led to a decrease in the ratio of Cu-I/Cu-II (1915 cm^{-1} / 1895 cm^{-1}) and an increase in the population of Cu^{+} sites (1811 cm^{-1}, attributable to reduced Cu-II type sites). In fact, above a Cu/Al ratio of 0.5, population of these highly reducible square planar Cu^{2+} sites (associated with a single AlO_4^- site) became dominant. The shift in speciation of Cu corresponds with the drop in methane conversion and methanol selectivity (shown in Table 1) at Cu/Al > 0.5.

To better understand the mechanism by which Cu^{2+} sites affect both methane conversion and methanol selectivity, EPR spectroscopy radical trapping studies were performed. EPR revealed that significant quantities of hydroxyl radicals are produced over 2.5 % Cu/ZSM-5 (23) (Figure 8a). This is surprising, as previous studies had correlated termination of such radicals over Cu sites with high methanol selectivity. Spectra for reactions over 2.5 % Cu/ ZSM-5 where SiO_2/Al_2O_3 = 30 and 280 are shown in Figures 8b and 8c. Spectrum 8b is consistent with previous EPR DMPO trapping studies over the same catalyst [31], showing weak signals, which were previously attributed to superoxide (O_2^-) radicals. As previously discussed, the hydrophobic/ hydrophilic nature of the represented ZSM-5 isomorphs differ significantly. To further explore the relationship between supported species and radicals generated, without varying hydrophobicity, the spin trap (DMPO) was added to methane oxidation reactions catalysed by 1.25 % Cu/ZSM-5 (30). This catalyst, with a Cu/Al ratio = 0.2 showed significantly higher methane conversion rates (3.3 mol kg_{cat}^{-1} h^{-1}) and methanol selectivity (86.0 %) than 2.5 % Cu/ZSM-5 (30) (Si/Al = 0.59, 0.6 mol kg_{cat}^{-1} h^{-1}, 78.5 % methanol selectivity) at near iso-conversion of H_2O_2 (Table 1, Entries 2 and 11). The EPR spectrum for methane oxidation catalysed by 1.25 % Cu/ZSM-5 (30) is shown in Figure 9a. This is comparable to that of 2.5 % Cu/ZSM-5 (23) in Figure 8a, showing significant DMPO-·OH adduct formation. EPR studies therefore suggest that at a Cu/Al of < 0.5, supported Cu/ZSM-5 catalysts behave differently to the previously reported 2.5 % Cu/ZSM-5 (30) (Cu/Al = 0.59) system. When the Cu/Al is less than 0.5 (Cu-I species dominant), addition of copper has a beneficial effect upon both methane conversion rates and methanol selectivity, with EPR radical trapping studies showing these systems to contain appreciable quantities of hydroxyl radicals. These data suggest that (i) ·OH are generated at and relatively stable over Cu-I sites and that either (ii) Cu-I species act as active sites for selective methane oxidation or (iii) Cu-I sites propagate generation of ·OH, with methane activation occurring on a secondary active site within the catalyst. Conversely, the previously reported DFT- derived mechanism for ZSM-5 catalysed methane oxidation with H_2O_2 involved a concerted, molecular active site with no input of oxygen based radicals [26].

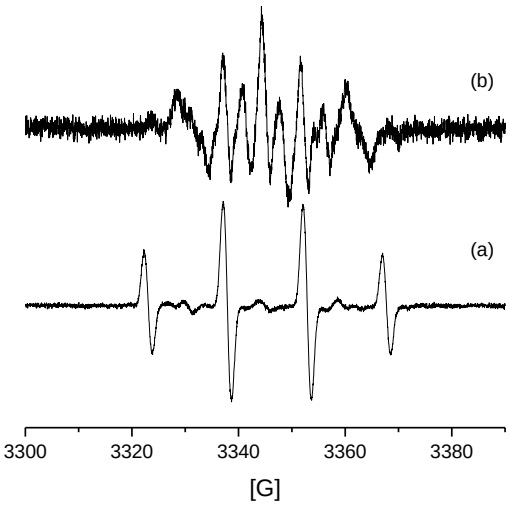

Figure 9 DMPO spin- trapping data obtained during a methane oxidation reaction catalysed by (a) 1.25 % Cu/ZSM-5 (30) and (b) 2.5 % Cu/ZSM-5 (30) Reaction conditions; 27 mg catalyst, 50 ^{o}C, 5 min, [H_2O_2] = 0.5 M (5,000 µmol), 1500 rpm P(CH_4) = 30 bar.

Table 2 Catalytic data for ethane oxidation catalysed by Cu/ZSM-5 of varied SiO_2/Al_2O_3 and Cu/Al ratios.

Entry	SiO_2/ Al_2O_3	wt% Cu	Cu/Al ratio	χ C_2H_6 / %[a]	Product Selectivities / %									χ H_2O_2 / %
					CH_3COOH	EtOH	CH_3CHO	EtOOH	MeOOH	MeOH	HCOOH	C_2H_4	CO_2	
1	23	2.5	0.41	0.11	6.0	30.2	8.2	0.6	0.0	0.1	0.0	51.7	0.9	33.2
2	30	2.5	0.59	0.07	13.4	34.1	13.7	1.0	1.6	6.2	0.0	27.1	2.4	33.9
3	50	2.5	0.76	0.04	19.0	19.0	44.4	3.2	4.0	1.6	4.0	0.9	2.7	18.4
4	280	2.5	4.08	0.06	23.2	10.5	47.6	7.0	4.1	1.7	2.3	0.6	2.0	31.9
5	23	0	n.a	0.01	4.9	34.6	14.8	14.8	0.00	5.0	4.9	10.6	10.0	14.2
6	23	0.4	0.07	0.08	9.3	22.8	5.1	4.2	1.3	1.3	0.4	53.4	2.2	6.9
7	23	1.25	0.20	0.10	7.7	25.7	4.9	2.8	0.7	1.4	0.4	55.0	1.5	14.1
8	23	5.0	0.82	0.04	18.6	38.7	6.2	13.9	2.3	1.6	0.8	14.3	3.6	33.7
9	30	0	n.a	0.06	17.7	24.0	36.7	10.1	2.5	2.5	2.5	2.3	1.3	25.3
10	30	0.4	0.09	0.20	14.6	24.7	7.7	0.4	0.7	3.7	2.4	45.0	0.7	17.8
11	30	1.25	0.29	0.23	14.1	27.5	7.9	2.1	0.3	3.2	2.8	41.6	0.5	14.0
12	30	5.0	1.18	0.06	20.4	24.0	12.0	9.6	3.0	3.6	1.8	22.6	2.9	33.2
13[a]	n/a	2.5	n/a	0.09	16.4	23.9	35.8	5.2	1.5	1.5	1.1	12.8	1.5	47.1

[a] Conversion based on carbon. [b] 2.5% Cu/Silicalite-1 prepared by CVI. Test conditions; 27 mg catalyst, 0.5 h, $P(C_2H_6)$ = 20 bar, 50 °C, 1500 rpm, $[H_2O_2]$ = 0.5 M (5000 μmol).

To further study the structure- function relationships in these Cu-MFI catalysts, they were assessed for activity in ethane oxidation, which our previous studies showed to be mediated at least in part by oxygen-based radicals [27]. Trends in Table 2 are consistent with those in Table 1. At a fixed 2.5 wt. % Cu loading, ZSM-5 (23) affords the highest rate of C_2H_6 conversion (1.6 mol kg_{cat}^{-1} h^{-1}) and relatively high ethene selectivity (51.7 %). These metrics decrease with increasing SiO_2/Al_2O_3. As with methane, for a specific ZSM-5 support, the rate of ethane conversion increases with increasing Cu loading until Cu/Al = 0.5. Ethane conversion then decreases significantly upon over- exchange with Cu, as does ethene selectivity (from 55.0 % to 14.3% in Table 2 Entries 7 and 8). Trends in selectivity/ reaction rate are observed at longer times on line (Figure S5). This further implicates ethene as a primary product of ethane oxidation under these reaction conditions.

When assessed for activity in the partial oxidation of propane, under similarly mild conditions, trends were again consistent with those in Tables 1 and 2. Indeed Entries 1-4 in Table 3 show similar trends to entries 1-4 in Table 2. At a fixed 2.5 wt. % Cu loading, ZSM-5 (SiO_2/Al_2O_3 = 23) showed the highest propane conversion (0.39 %) and relatively high alkene selectivity ($S(C_3H_6$ = 59.7)). Both metrics decreased at a Cu/Al > 0.5, with 2.5 % Cu/ZSM-5 (30) affording 0.26 % propane conversion and markedly lower propene selectivity (20.8 %). At longer times on line, and consequently higher ethane conversion, the same trends in ethane conversion rate and reaction selectivity were observed as shown in Figure S4. From a mechanistic perspective it is interesting to note that whilst 2.5% Cu/Silicalite-1 showed comparable propane conversion to 2.5 % Cu/ZSM-5 (23) (χ propane = 0.36 %), no propene was observed in the GC-FID (sensitive to < 1 ppm), with selectivity favouring IPA (38.4 % selectivity) and the rate of H_2O_2 conversion was an order of magnitude greater. As with ethane, the catalytic oxidation of propane under these reaction conditions was previously shown to be at least partially dependent upon oxygen-based radicals [32, 72].

The catalysis and characterisation studies reported herein show strong trends between Cu/ZSM-5 catalysed oxidative upgrading of C_1-C_3 alkanes in water using hydrogen peroxide as oxidant. It is clear that Cu speciation plays a key role in achieving high primary product selectivity, be it to methanol, ethene or propene. Whilst H-ZSM-5 (SiO_2/Al_2O_3 = 30) shows the highest intrinsic activity of proton form zeolites, following modification with Cu, ZSM-5 (23) shows appreciable rates of alkane oxidation and, crucially, high reaction selectivity. The production of ethene/ propene in this way using H_2O_2 is academically interesting, and provides mechanistic insight into the performance of these catalysts under methane oxidation conditions. The performance of the copper catalysts exceeds that of previous reports [26, 30], crucially due to use of catalysts with a Cu/Al ratio of < 0.5. Spectroscopic and temperature programmed studies show that this favours formation of Cu-I sites and this correlates with enhanced catalyst productivity (relative to the parent proton-form of the zeolite). Over exchanging ZSM-5 (Cu/Al > 0.5) leads to population of spectroscopically distinct Cu-II sites. This shift from a majority of Cu-I to Cu-II species is associated with: lower rates of alkane oxidation, lower primary product selectivity and increased rates of H_2O_2 conversion. This relationship between Cu/Al (at fixed 2.5 wt. % Cu) and reaction productivity for the catalytic oxidation of short chain alkanes is illustrated in Figure 10. It is therefore clear that Cu-I sites have bi-functionality:

Table 3 Catalytic data for propane oxidation catalysed by 2.5% Cu/ MFI zeolites of varied SiO_2/Al_2O_3 ratios.

Entry	SiO_2/ Al_2O_3	χ C_3H_8 / %	C_3 Selectivities/ %				C_2 Selectivities				C_1 Selectivities				χ H_2O_2 / %
			Acetone	IPA	PrOH	Propanoic Acid	C_3H_6	Acetic Acid	EtOH	C_2H_6	C_2H_4	MeOH	Formic Acid	CO_2	Other[a]	
1	23	0.39	8.4	0.0	18.6	2.3	59.7	1.1	0.0	5.8	1.7	1.0	0.1	1.1	0.4	2.7
2	30	0.26	9.3	19.8	18.8	3.2	20.8	1.0	1.4	12.6	2.1	2.5	4.0	1.2	3.2	1.7
3	50	0.06	18.6	0.0	6.9	0.0	9.7	6.7	7.4	33.3	0.3	1.9	0.0	9.4	5.8	8.6
4	280	0.06	25.3	0.0	19.6	0.0	11.8	7.7	17.7	2.3	0.6	4.4	0.0	5.4	5.3	14.8
5[b]	n.a	0.36	19.7	38.4	18.3	7.9	0.0	0.0	0.0	7.6	1.0	0.6	4.2	1.5	0.9	26.5

Test conditions; 27 mg catalyst, 0.5 h, $P(C_3H_8)$ = 4 bar, P(Total/ C_3H_8/ Helium) = 20 bar, 50 °C, 1500 rpm, $[H_2O_2]$ = 0.5 M (5000 μmol). [a] Selectivity ($CO + CH_4$), [b] Catalyst – 2.5% Cu/Silicalite-1 (CVI)

suppressing over-oxidation of methanol to formic acid and increasing catalyst productivity. Once population of Cu-II sites becomes preferable, over Cu-I, further oxidation of methanol is still suppressed, though these sites are associated with decreased rates of methane oxidation coupled with increased H_2O_2 conversion rates.

Conclusions

Cu/ZSM-5 catalysts are active for liquid phase oxidative upgrading of short chain alkanes, with H_2O_2 under mild conditions. In the present work, we have shown that both the activity and selectivity of these catalysts correlates strongly with the Cu/Al ratio, and thereby the degree of ion exchange. Catalytic performance correlates strongly with the speciation of exchanged Cu- species as determined by characterisation studies. Optimal conversion and primary product selectivity (that is; methanol, ethene and propene for C_1, C_2 and C_3 alkanes respectively) were observed when the speciation of Cu is dominated by so- called Cu-I sites. These are favoured when the zeolite catalyst's Cu/Al ratio is below the level of total exchange (Cu/Al < 0.5). Once over-exchanged, catalyst performance and selectivity decreases, and this coincides with formation of spectroscopically distinct, Cu-II sites. This study provides insight as to the nature of the Cu sites within ZSM-5 that afford the high methanol selectivities, which have previously been reported and goes further, identifying Cu sites that are capable of effecting increased reaction yields. Indeed, 1.25 wt. % Cu/ZSM-5 (23) yielded 49.86 µmol MeOH in 0.5 h. This equated to 96.1 % selectivity towards methanol and a methanol productivity of 3.7 mol $kg_{cat}^{-1}h^{-1}$. Furthermore, accounting for the intrinsic activity of the ZSM-5 (23) support, this catalyst showed an apparent TOF (based on Cu) of 16.9 mol $_{\text{methane converted}}$ $mol_{Cu}^{-1}h^{-1}$. Owing to the complexity of reactions between Cu and H_2O_2, the specific mechanisms through which copper sites effect the radical- reactions involved has not been addressed in this article but will form the basis for a future publication.

Acknowledgements

We thank Cardiff University for financial support. We would like to thank the Cardiff Electron Microscopy Facility for the HRTEM analysis.

Experimental

Catalyst Preparation

Supported metal catalysts were prepared by chemical vapour impregnation (CVI). This methodology has previously been discussed in detail [27, 73].

NH_4 ZSM-5 (*Zeolyst*) was calcined in a flow of air (550 °C, 20 °C min^{-1}, 3h) to yield H-ZSM-5. The proton form zeolite was then either; activated in static air prior to testing (550 °C, 20 °C, 3h), or impregnated with Cu via chemical vapour impregnation. The procedure for preparation of 2.5 wt% Cu/ZSM-5 through CVI is as follows; a known mass of H-ZSM-5 (typically 3.5 g) was dried at 150 °C for 2 h under continuous vacuum. Once dried, the desired mass of H-ZSM-5 (1.95 g) was added to a Schlenk flask and Cu(II) acetylacetonate ($Cu(acac)_2$) (*Sigma Aldrich*, 99.9% purity, 0.206 g, 0.787 mmol) added. Following physical mixing of the metal precursor and zeolite, the dry mixture was heated to 140 °C under continuous vacuum (*ca.* 10^{-3} mbar) for 1 h. The sample was then allowed to cool to ambient temperature and calcined (550 °C, 20 °C min^{-1}, 3h) in static air.

Alkane oxidation

Catalyst performance assessed in a 50 mL Teflon lined Parr autoclave reactor. A procedure for ethane oxidation reactions is described here. The reactor was charged with H_2O_2 (0.5 M, 5000 µmol) and catalyst added (27 mg). Once sealed, the reactor was purged 3 times with the reactant gas (20 bar) to remove residual gasses. The reactor was then charged with one of; methane (30 bar, CH_4, *Air Products* 99.9%, 0.03 mol CH_4), ethane (20 bar C_2H_6, *Air Products* 99.9%, 0.02 mol C_2H_6) or propane (*P* C_3H_8 = 4 bar, *P* He = 16 bar, *BOC*, 0.004 mol). The reactor was then heated to the reaction temperature (50 °C) under vigorous stirring (1500 rpm). Once the set point temperature was reached, the reaction was carried out for the desired time. The autoclave was then cooled to *ca.* 10 °C to minimise loss of volatile products. Post reaction, unreacted hydrogen peroxide was quantified through titration with acidified Ce $(SO_4)_2$ (8 x 10^{-3} mol dm^{-3}) of known concentration, with a Ferroin indicator. Aqueous products were quantified with solvent suppressed ^{1}H NMR at ambient temperature on a Bruker Ultrashield 500 MHz spectrometer using a TMS/ $CDCl_3$ internal standard. Gaseous products were quantified using a *Varian 450*-GC fitted with a CP-Sil 5CB capillary column (50m length, 0.32mm diameter, carrier gas = He), a methaniser unit and both FID and TCD detectors.

For EPR radical trapping studies, the reactor was charged with methane as previously described, with the addition of 5,5-Dimethyl-1-pyrroline N-oxide (0.05 g, *Sigma Aldrich*, > 97%). Reactions were carried out for 5 min at 50 °C, after which time the reactor was depressurised, opened and solution filtered prior to analysis. EPR spectra were collected at 298 K in a high sensitivity cavity (Bruker ER 4119 HS) Bruker EMX spectrometer, field modulation 100 kHz, microwave power 1 mW.

Catalyst Characterisation

H_2-TPR was carried out using a TPDRO 1100 series analyser. Samples (equivalent to 0.03 mmol Cu) were pre-treated for 1 h at 130 °C (20 °C min^{-1}) in a flow of Argon (20 ml min^{-1}). Following this the gas flow was changed to 10% H_2 / Argon and the temperature was ramped to 800 °C (10 °C min^{-1}). Hydrogen uptake was monitored using a TCD.

NH_3-TPD was carried out using a CHEMBET TPR/TPD chemisorption analyser, *Quantachrome Industries* fitted with a TCD. 50 mg of sample was pre-treated for 1 h at 130 °C (15 °C min^{-1}) in a flow of helium (80 ml min^{-1}). The sample was then cooled to ambient temperature and ammonia flowed through for 20 min to ensure saturation. The system was then heated 1 h at 100 °C (15 °C min^{-1}) under a flow of helium (80 ml min^{-1}) to remove physisorbed ammonia. Subsequently, chemisorbed ammonia was desorbed by heating to 900 °C (15 °C min^{-1}) in a flow of helium (80 ml min^{-1}) during which period desorbed ammonia was monitored using a TCD, current 180 mV, attenuation 1.

TEM images were collected on a JEOL JEM-2100 transmission electron microscope fitted with a LaB_6 filament. Samples were prepared by dispersing powdered catalyst in high purity ethanol, before adding a drop

of the suspension to porous carbon film supported by a meshed copper TEM grid.

IR spectra were collected on a Bruker Tensor 27 spectrometer fitted with a liquid N_2 - cooled MCT detector. Samples were housed in a Praying Mantis high temperature diffuse reflection environmental reaction chamber (HVC-DRP-4) fitted with calcium fluoride windows. For characterisation of the hydroxyl region, samples were pre-treated prior to acquisition by heating at 200 ^oC (10 ^oC min^{-1}) in a flow of N_2 (10 ml min^{-1}) for 1 h. Scans were collected across the range 4000 cm^{-1} to 1500 cm^{-1}, 4 cm^{-1} resolution, 64 scans against a KBr background. For NO adsorption studies, samples were pre-treated in N_2 by heating for 10 min at 500 ^oC (100 ^oC min^{-1}). The background was then acquired at room temperature. NO (5000 ppm in N_2, 1 bar) was then flowed over the sample at ambient conditions, with spectra collected at 1 min intervals over a 20 min period.

N_2 isotherms were collected on a Micromeritics 3Flex. Samples (ca. 0.020 g) were degassed (150 ^oC, 6 h) prior to analysis. Analyses were carried out at 77 K with P_0 measured continuously. Free space was measured post- analysis with He. Pore size analysis was carried out using Micromeritics 3Flex software, N_2-Cylindrical Pores- Oxide Surface Model.

Keywords: Selective Oxidation • Methane • Ethane • Propane • Cu/ZSM-5

[1] S.J. Blanksby, G.B. Ellison, Bond dissociation energies of organic molecules, Accounts Chem. Res., 36 (2003) 255-263.

[2] M.A. Pena, J.P. Gomez, J.L.G. Fierro, New catalytic routes for syngas and hydrogen production, Appl. Catal., A, 144 (1996) 7-57.

[3] J.H. Jones, The Cativa™ Process for the Manufacture of Acetic Acid, Platinum Metals Rev, 44 (2000) 94-105.

[4] N. Yoneda, S. Kusano, M. Yasui, P. Pujado, S. Wilcher, Recent advances in processes and catalysts for the production of acetic acid, Appl. Catal. A-Gen., 221 (2001) 253-265.

[5] W. Bertleff, M. Roeper, X. Sava, Carbonylation, in: Ullmann's Encyclopedia of Industrial Chemistry, Wiley-VCH Verlag GmbH & Co. KGaA, 2000.

[6] N. Rahimi, R. Karimzadeh, Catalytic cracking of hydrocarbons over modified ZSM-5 zeolites to produce light olefins: A review, Applied Catalysis A: General, 398 (2011) 1-17.

[7] J. Colby, D.I. Stirling, H. Dalton, Soluble Methane Mono-Oxygenase of Methylococcus-Capsulatus-(Bath)- ability to oxygenate normal alkanes, normal- alkenes, ethers and alicyclic, aromatic and heterocyclic-compounds, Biochem. J., 165 (1977) 395-402.

[8] A.A. Shteinman, The role of metal-oxygen intermediates in biological and chemical monooxygenation of alkanes, Russ. Chem. Bull., 50 (2001) 1795-1810.

[9] J. Cook, B. Ellis, P. Howard, M.D. Jones, S.J. Kitchen, Process for the production of acetic acid, in, Nixon & Vanderhye, 2001.

[10] K. Karim, M. Al-Hazmi, A. Khan, Catalysts for the oxidation of ethane to acetic acid, methods of making and using the same in: S.B.I. CORP (Ed.), 2000.

[11] N. Mizuno, W.C. Han, T. Kudo, Selective oxidation of ethane, propane, and isobutane catalyzed by copper-containing Cs2.5H1.5PVMo11O40 under oxygen-poor conditions, Journal of Catalysis, 178 (1998) 391-394.

[12] J.B. Moffat, Conversion of C-2-C-5 alkanes on heteropoly oxometalates, Appl. Catal. A-Gen., 146 (1996) 65-86.

[13] S.T. Oyama, G.A. Somorjai, Effect of structure in selective oxide catalysis-oxidation of ethanol and ethane on vanadium-oxide, Journal of Physical Chemistry, 94 (1990) 5022-5028.

[14] Y. Wang, K. Otsuka, Partial Oxidation of Ethane by Reductively Activated Oxygen over Iron Phosphate Catalyst, Journal of Catalysis, 171 (1997) 106-114.

[15] J.J. Bravo-Suárez, K.K. Bando, T. Fujitani, S.T. Oyama, Mechanistic study of propane selective oxidation with H2 and O2 on Au/TS-1, Journal of Catalysis, 257 (2008) 32-42.

[16] J.F. Brazdil, R.J. George, B.I. Rosen, Mixed metal oxide catalyst composition and process for the selective oxidation of ethane and/or ethylene to acetic acid, in, BP Chemicals Limited, UK . 2004, pp. 17 pp.

[17] K. Miki, T. Furuya, Catalytic hydroxylation of alkanes by immobilized mononuclear iron carboxylate, Chemical Communications, (1998) 97-98.

[18] G.B. Shul'pin, G.V. Nizova, Y.N. Kozlov, L. Gonzalez Cuervo, G. Süss-Fink, Hydrogen Peroxide Oxygenation of Alkanes Including Methane and Ethane Catalyzed by Iron Complexes in Acetonitrile, Advanced Synthesis & Catalysis, 346 (2004) 317-332.

[19] N. Basickes, T.E. Hogan, A. Sen, Radical-Initiated Functionalization of Methane and Ethane in Fuming Sulfuric Acid, Journal of the American Chemical Society, 118 (1996) 13111-13112.

[20] T. Hogan, A. Sen, High-Yield, Radical-Initiated Oxidative Functionalization of Ethane by Perfluorocarboxylic Acid Anhydrides. Role of Metal Ions in Catalytic Alkane Oxidations in the Presence of Perfluorocarboxylic Acid Anhydrides, Journal of the American Chemical Society, 119 (1997) 2642-2646.

[21] A. Sen, M.A. Benvenuto, M. Lin, A.C. Hutson, N. Basickes, Activation of Methane and Ethane and Their Selective Oxidation to the Alcohols in Protic Media, Journal of the American Chemical Society, 116 (1994) 998-1003.

[22] B.G. Hashiguchi, M.M. Konnick, S.M. Bischof, S.J. Gustafson, D. Devarajan, N. Gunsalus, D.H. Ess, R.A. Periana, Main-Group Compounds Selectively Oxidize Mixtures of Methane, Ethane, and Propane to Alcohol Esters, Science, 343 (2014) 1232-1237.

[23] R.A. Periana, D.J. Taube, S. Gamble, H. Taube, T. Satoh, H. Fujii, Platinum Catalysts for the High-Yield Oxidation of Methane to a Methanol Derivative, Science, 280 (1998) 560-564.

[24] K.A. Dubkov, V.I. Sobolev, E.P. Talsi, M.A. Rodkin, N.H. Watkins, A.A. Shteinman, G.I. Panov, Kinetic isotope effects and mechanism of biomimetic oxidation of methane and benzene on FeZSM-5 zeolite, Journal of Molecular Catalysis a-Chemical, 123 (1997) 155-161.

[25] G.I. Panov, V.I. Sobolev, K.A. Dubkov, V.N. Parmon, N.S. Ovanesyan, A.E. Shilov, A.A. Shteinman, Iron complexes in zeolites as a new model of methane monooxygenase, React Kinet Catal Lett, 61 (1997) 251-258.

[26] C. Hammond, M.M. Forde, M.H. Ab Rahim, A. Thetford, Q. He, R.L. Jenkins, N. Dimitratos, J.A. Lopez-Sanchez, N.F. Dummer, D.M. Murphy, A.F. Carley, S.H. Taylor, D.J. Willock, E.E. Stangland, J. Kang, H. Hagen, C.J. Kiely, G.J. Hutchings, Direct Catalytic Conversion of Methane to Methanol in an Aqueous Medium by using Copper-Promoted Fe-ZSM-5, Angewandte Chemie International Edition, 51 (2012) 5129-5133.

[27] M.M. Forde, R.D. Armstrong, C. Hammond, Q. He, R.L. Jenkins, S.A. Kondrat, N. Dimitratos, J.A. Lopez-Sanchez, S.H. Taylor, D. Willock, C.J. Kiely, G.J. Hutchings, Partial Oxidation of Ethane to Oxygenates Using Fe- and Cu-Containing ZSM-5, Journal of the American Chemical Society, 135 (2013) 11087-11099.

[28] A.K.M.L. Rahman, M. Kumashiro, T. Ishihara, Direct synthesis of formic acid by partial oxidation of methane on H-ZSM-5 solid acid catalyst, Catalysis Communications, 12 (2011) 1198-1200.

[29] A.K.M.L. Rahman, R. Indo, H. Hagiwara, T. Ishihara, Direct conversion of ethane to acetic acid over H-ZSM-5 using H2O2 in aqueous phase, Applied Catalysis A: General, 456 (2013) 82-87.

[30] C. Hammond, N. Dimitratos, R.L. Jenkins, J.A. Lopez-Sanchez, S.A. Kondrat, M. Hasbi ab Rahim, M.M. Forde, A. Thetford, S.H. Taylor, H. Hagen, E.E. Stangland, J.H. Kang, J.M. Moulijn, D.J. Willock, G.J. Hutchings, Elucidation and Evolution of the Active Component within Cu/Fe/ZSM-5 for Catalytic Methane Oxidation: From Synthesis to Catalysis, ACS Catalysis, 3 (2013) 689-699.

[31] C. Hammond, R.L. Jenkins, N. Dimitratos, J.A. Lopez-Sanchez, M.H. ab Rahim, M.M. Forde, A. Thetford, D.M. Murphy, H. Hagen, E.E. Stangland, J.M. Moulijn, S.H. Taylor, D.J. Willock, G.J. Hutchings, Catalytic and Mechanistic Insights of the Low-Temperature Selective Oxidation of

Methane over Cu-Promoted Fe-ZSM-5, Chemistry – A European Journal, 18 (2012) 15735-15745.
[32] V. Peneau, G. Shaw, R.D. Armstrong, R.L. Jenkins, N. Dimitratos, S.H. Taylor, H.W. Zanthoff, S. Peitz, G. Stochniol, G.J. Hutchings, The partial oxidation of propane under mild aqueous conditions with H_2O_2 and ZSM-5 catalysts, Catalysis Science & Technology, (2016).
[33] H. Borchert, U. Dingerdissen, J. Weiguny, Process and palladium-containing catalyst for the selective production of acetic acid by the gas-phase oxidation of ethane and/or ethylene, in, Hoechst A.-G., Germany . 1997, pp. 6 pp.
[34] K.-I. Sano, H. Uchida, S. Wakabayashi, A new process for acetic acid production by direct oxidation of ethylene, Catal. Surv. Jpn., 3 (1999) 55-60.
[35] B. Wichterlova, J. Dedecek, Z. Sobalik, A. Vondrova, K. Klier, On the Cu site in ZSM-5 active in decomposition of NO: Luminescence, FTIR study, and redox properties, Journal of Catalysis, 169 (1997) 194-202.
[36] B. Wichterlová, Z. Sobalík, J. Dědeček, Cu ion siting in high silica zeolites. Spectroscopy and redox properties, Catalysis Today, 38 (1997) 199-203.
[37] B. Wichterlova, Z. Sobalik, A. Vondrova, Differences in the structure of copper active sites for decomposition and selective reduction of nitric oxide with hydrocarbons and ammonia, Catalysis Today, 29 (1996) 149-153.
[38] A.N. Pham, G. Xing, C.J. Miller, T.D. Waite, Fenton-like copper redox chemistry revisited: Hydrogen peroxide and superoxide mediation of copper-catalyzed oxidant production, Journal of Catalysis, 301 (2013) 54-64.
[39] J.K. Kim, I.S. Metcalfe, Investigation of the generation of hydroxyl radicals and their oxidative role in the presence of heterogeneous copper catalysts, Chemosphere, 69 (2007) 689-696.
[40] E.A. Urquieta-González, L. Martins, R.P.S. Peguin, M.S. Batista, Identification of Extra-Framework Species on Fe/ZSM-5 and Cu/ZSM-5 Catalysts Typical Microporous Molecular Sieves with Zeolitic Structure, Materials Research, 5 (2002) 321-327.
[41] C. TorreAbreu, M.F. Ribeiro, C. Henriques, G. Delahay, Characterisation of CuMFI catalysts by temperature programmed desorption of NO and temperature programmed reduction. Effect of the zeolite Si/Al ratio and copper loading, Applied Catalysis B-Environmental, 12 (1997) 249-262.
[42] J.A. Sullivan, J. Cunningham, M.A. Morris, K. Keneavey, Conditions in which Cu-ZSM-5 outperforms supported vanadia catalysts in SCR of NOx by NH3, Applied Catalysis B-Environmental, 7 (1995) 137-151.
[43] G. Delahay, B. Coq, L. Broussous, Selective catalytic reduction of nitrogen monoxide by decane on copper-exchanged beta zeolites, Appl. Catal., B, 12 (1997) 49-59.
[44] R. Bulanek, B. Wichterlova, Z. Sobalik, J. Tichy, Reducibility and oxidation activity of Cu ions in zeolites - Effect of Cu ion coordination and zeolite framework composition, Applied Catalysis B-Environmental, 31 (2001) 13-25.
[45] C. Dossi, A. Fusi, S. Recchia, R. Psaro, G. Moretti, Cu–ZSM-5 (Si/Al=66), Cu–Fe–S-1 (Si/Fe=66) and Cu–S-1 catalysts for NO decomposition: preparation, analytical characterization and catalytic activity, Microporous and Mesoporous Materials, 30 (1999) 165-175.
[46] C. Torre-Abreu, M.E. Ribeiro, C. Henriques, G. Delahay, NO TPD and H-2-TPR studies for characterisation of CuMOR catalysts the role of Si/Al ratio, copper content and cocation, Applied Catalysis B-Environmental, 14 (1997) 261-272.
[47] T. Beutel, J. Sarkany, G.D. Lei, J.Y. Yan, W.M.H. Sachtler, Redox Chemistry of Cu/ZSM-5, J. Phys. Chem., 100 (1996) 845-851.
[48] B. Hunger, J. Hoffmann, O. Heitzsch, M. Hunger, Temperature-programmed desorption (TPD) of ammonia from HZSM-5 zeolites, J. Therm. Anal., 36 (1990) 1379-1391.
[49] K.H. Schnabel, C. Peuker, B. Parlitz, E. Loffler, U. Kurschner, H. Kriegsmann, IR- spectroscopic investigation of the adsorption of NH_3 and H_2O to Na-ZSM-5 and H-ZSM-5, Zeitschrift Fur Physikalische Chemie-Leipzig, 268 (1987) 225-234.
[50] H. Dang Lanh, D. Thi Thuy Hanh, J. Engeldinger, M. Schneider, J. Radnik, M. Richter, A. Martin, TPR investigations on the reducibility of Cu supported on Al2O3, zeolite Y and SAPO-5, Journal of Solid State Chemistry, 184 (2011) 1915-1923.
[51] C. Ding, X. Wang, X. Guo, S. Zhang, Characterization and catalytic alkylation of hydrothermally dealuminated nanoscale ZSM-5 zeolite catalyst, Catal. Commun., 9 (2007) 487-493.
[52] R.Q. Long, R.T. Yang, Temperature-programmed desorption/surface reaction (TPD/TPSR) study of Fe-exchanged ZSM-5 for selective catalytic reduction of nitric oxide by ammonia, Journal of Catalysis, 198 (2001) 20-28.
[53] M. Iwasaki, K. Yamazaki, K. Banno, H. Shinjoh, Characterization of Fe/ZSM-5 DeNOx catalysts prepared by different methods: Relationships between active Fe sites and NH3-SCR performance, J. Catal., 260 (2008) 205-216.
[54] B. Dou, G. Lv, C. Wang, Q. Hao, K. Hui, Cerium doped copper/ZSM-5 catalysts used for the selective catalytic reduction of nitrogen oxide with ammonia, Chemical Engineering Journal, 270 (2015) 549-556.
[55] F.W. Schuetze, F. Roessner, J. Meusinger, H. Papp, Hydrogen/deuterium exchange on dealuminated H-ZSM-5 zeolites studied by time resolved FTIR spectroscopy, Stud. Surf. Sci. Catal., 112 (1997) 127-134.
[56] B.J. Adelman, T. Beutel, G.D. Lei, W.M.H. Sachtler, Mechanistic Cause of Hydrocarbon Specificity over Cu/ZSM-5 and Co/ZSM-5 Catalysts in the Selective Catalytic Reduction of NOx, Journal of Catalysis, 158 (1996) 327-335.
[57] M. Iwamoto, H. Furukawa, Y. Mine, F. Uemura, S. Mikuriya, S. Kagawa, Copper(II) ion-exchanged ZSM-5 zeolites as highly active catalysts for direct and continuous decomposition of nitrogen monoxide, J. Chem. Soc., Chem. Commun., (1986) 1272-1273.
[58] R. Burch, S. Scire, Selective catalytic reduction of nitric oxide with ethane and methane on some metal exchanged ZSM-5 zeolites, Appl. Catal., B, 3 (1994) 295-318.
[59] B. Wichterlova, J. Dedecek, Z. Sobalik, Cu coordination in high silica zeolites. Effect of the framework Al local siting, Elsevier Science Publ B V, Amsterdam, 1995.
[60] I. Othman Ali, Preparation and characterization of copper nanoparticles encapsulated inside ZSM-5 zeolite and NO adsorption, Materials Science and Engineering: A, 459 (2007) 294-302.
[61] Y. Kuroda, R. Kumashiro, T. Yoshimoto, M. Nagao, Characterization of active sites on copper ion-exchanged ZSM-5-type zeolite for NO decomposition reaction, Physical Chemistry Chemical Physics, 1 (1999) 649-656.
[62] J. Dedecek, Z. Sobalik, Z. Tvaruazkova, D. Kaucky, B. Wichterlova, Coordination of Cu Ions in High-Silica Zeolite Matrixes. Cu+ Photoluminescence, IR of NO Adsorbed on Cu2+, and Cu2+ ESR Study, The Journal of Physical Chemistry, 99 (1995) 16327-16337.
[63] N. Beznis, B. Weckhuysen, J. Bitter, Cu-ZSM-5 Zeolites for the Formation of Methanol from Methane and Oxygen: Probing the Active Sites and Spectator Species, Catalysis Letters, 138 (2010) 14-22.
[64] R. Kefirov, A. Penkova, K. Hadjiivanov, S. Dzwigaj, M. Che, Stabilization of Cu+ ions in BEA zeolite: Study by FTIR spectroscopy of adsorbed CO and TPR, Microporous and Mesoporous Materials, 116 (2008) 180-187.
[65] J. Dedecek, L. Capek, P. Sazama, Z. Sobalik, B. Wichterlova, Control of metal ion species in zeolites by distribution of aluminium in the framework: From structural analysis to performance under real conditions of SCR-NOx and NO, N2O decomposition, Appl. Catal., A, 391 (2011) 244-253.
[66] S.C. Larsen, A. Aylor, A.T. Bell, J.A. Reimer, Electron Paramagnetic Resonance Studies of Copper Ion-Exchanged ZSM-5, J. Phys. Chem., 98 (1994) 11533-11540.
[67] T. Kawai, K. Tsutsumi, Evaluation of hydrophilic-hydrophobic character of zeolites by measurements of their immersional heats in water, Colloid Polym. Sci., 270 (1992) 711-715.
[68] S.M. Auerbach, K.A. Currado, P.K. Dutta, Handbook of Zeolites Science and Technology, Marcel Dekker Inc, New York, 2003.

[69] G.R.A. Johnson, N.B. Nazhat, R.A. Saadallanazhat, Reaction of the aquocopper(I) ion with hydrogen-peroxide- evidence against hydroxyl free- radical formation, J. Chem. Soc.-Chem. Commun., (1985) 407-408.
[70] J.F. Perez-Benito, Reaction pathways in the decomposition of hydrogen peroxide catalyzed by copper(II), Journal of Inorganic Biochemistry, 98 (2004) 430-438.
[71] T. Ozawa, A. Hanaki, The first ESR spin-trapping evidence for the formation of hydroxyl radical from the reaction of copper(II) complex with hydrogen peroxide in aqueous solution, J. Chem. Soc., Chem. Commun., (1991) 330-332.
[72] V. Peneau, R.D. Armstrong, G. Shaw, J. Xu, R.L. Jenkins, D.J. Morgan, N. Dimitratos, S.H. Taylor, H.W. Zanthoff, S. Peitz, G. Stochniol, Q. He, C.J. Kiely, G.J. Hutchings, The Low-Temperature Oxidation of Propane by using H2O2 and Fe/ZSM-5 Catalysts: Insights into the Active Site and Enhancement of Catalytic Turnover Frequencies, ChemCatChem, 9 (2017) 642-650.
[73] M.M. Forde, R.D. Armstrong, R. McVicker, P.P. Wells, N. Dimitratos, Q. He, L. Lu, R.L. Jenkins, C. Hammond, J.A. Lopez-Sanchez, C.J. Kiely, G.J. Hutchings, Light alkane oxidation using catalysts prepared by chemical vapour impregnation: tuning alcohol selectivity through catalyst pre-treatment, Chemical Science, 5 (2014) 3603-3616.

Entry for the Table of Contents (Please choose one layout)

Layout 1:

ARTICLE

Coppers vs Alkanes: Partial oxidation of short chain alkanes is a key challenge for the chemical sciences. Recently, a number of articles have reported C_1-C_3 alkane activation over Cu/ZSM-5 catalysts with H_2O_2. In this article, the specific Cu- sites which afford high product selectivity are identified through correlation of catalytic performance with the distribution of Cu-sites, as determined by spectroscopic and temperature- programmed analyses.

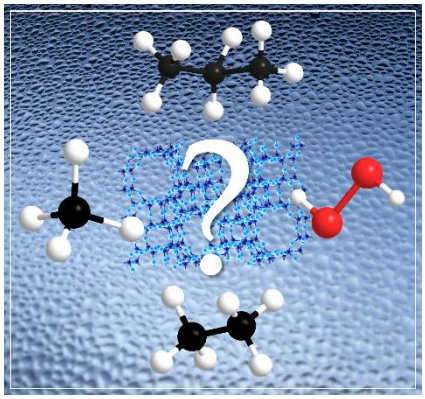

*Robert D. Armstrong, Virginie Peneau, Nadine Ritterskamp, Christopher J. Kiely, Stuart. H. Taylor and Graham J. Hutchings**

Page No. – Page No.

The role of copper speciation in the low temperature oxidative upgrading of short chain alkanes over Cu/ZSM-5 catalysts